Resonant two-photon ionization spectroscopy of jet-cooled Pt_2

Scott Taylor, George W. Lemire, Yoon Mi Hamrick, Zhenwen Fu, and Michael D. Morse
Department of Chemistry, University of Utah, Salt Lake City, Utah 84112

(Received 2 June 1988; accepted 25 July 1988)

The gas phase optical spectrum of jet-cooled Pt_2 has been investigated over the range of 11 300 to 26 300 cm^{-1} using resonant two-photon ionization spectroscopy in combination with time-of-flight mass spectrometry. Numerous vibronic bands are observed. Analysis of the data gives the location of some 26 excited electronic states, which are characterized by the frequencies of their origin bands, vibrational frequencies, and anharmonicities. Variation of the second color in a two-color resonant two-photon ionization scheme has determined the ionization threshold of Pt_2 to be 8.68 ± 0.02 eV. The observation of the onset of predissociation, characterized by a sharp drop in excited state lifetime, places the dissociation energy of Pt_2 at 3.14 ± 0.02 eV. In combination with the Pt atomic ionization potential of 8.8 ± 0.2 eV, these results give the bond strength of Pt_2^+ as $D_0(Pt - Pt^+) = 3.26 \pm 0.24$ eV. The strength of the chemical bond in Pt_2, as compared to Au_2, demonstrates that there are significant $5d$ contributions to the chemical bonding in Pt_2.

I. INTRODUCTION

Transition metal clusters form a class of chemical compounds which are of interest from both the experimental and theoretical points of view. The recent increase of interest in these species derives in part from advances in experimental methods, which have enabled ligand-free transition metal clusters to be produced in the gas phase, where they can be cooled to low internal energies. Once such species have been formed and cooled, their electronic and molecular architecture can be probed in detail using various elegant spectroscopies, including laser-induced fluorescence (LIF),[1-4] resonant two-photon ionization spectroscopy (R2PI),[5-7] resonant two-photon dissociation spectroscopy (R2PD),[8] and photoelectron spectroscopy (PES).[9-11] Alternatively, the reactivity of cold transition metal clusters can be investigated, potentially providing insights into the mechanisms of heterogeneous catalysis on transition metal surfaces.[12-16] In other studies, cold transition metal cluster ions can be accelerated to well-defined kinetic energies and collided with a variety of reaction partners, thereby providing much-needed thermochemical and kinetic information.[17-20]

Advances in theoretical methods, and the availability of supercomputers have also contributed greatly to the increased interest and understanding of transition metal clusters. Most of the sophisticated calculations of small transition metal molecules reported today would have been impossible a mere decade ago. As a result of these rapid improvements in theoretical methodology and computer power, and the simultaneous advances in experimental techniques, our knowledge and understanding of transition metal clusters is growing steadily. In view of the intrinsic difficulties associated with both the experimental and theoretical approaches to the complicated transition metal clusters, both disciplines are necessary for progress in understanding these interesting yet problematic molecules. The current state of our knowledge of the transition metal molecules has been reviewed in several recent publications.[21-27]

In this paper we report the results of spectroscopic investigations of the platinum dimer, Pt_2. Along with its congeners Pd_2 and Ni_2, this molecule is expected to possess a single sigma bond, with the remaining valence electrons arranged in two nd^9 cores. Among this series of molecules, the strength of the chemical bond and the splittings between the various angular momentum couplings of the nd^9 cores are sensitive measures of the detailed electronic structure. In contrast to the nickel dimer, d-orbital participation in the chemical bonding of Pd_2 and Pt_2 is expected to be of some importance because the nd contraction is less severe in the $4d$ and $5d$ transition metals than it is in the $3d$ metals.[22] On the other hand, the low bond strength of Pd_2, as measured by Knudsen effusion mass spectrometry,[28,29] has been rationalized[22] as arising from the high promotion energy (1.90 eV)[30] required to excite two ground state ($4d^{10}, {}^1S_0$) Pd atoms to the $4d^9 5s^1$ configuration, which is required for formation of a sigma bond. In addition to these promotion energy and nd contraction effects, chemical bonding in the Ni_2 series is influenced by relativistic effects and spin–orbit interaction, which are both quite large in Pt_2. Finally, correlation and exchange effects are quite important for an accurate description of the electronic structure in the transition metal dimers.

The theoretician who investigates the electronic structure and chemical bonding in Ni_2, Pd_2, and Pt_2 faces a severe challenge: in order to accurately calculate these open d-shell transition metal dimers he must include all of the effects mentioned in the previous paragraph. Moreover, all of these important effects must be calculated to a comparable level of accuracy, since the balance between them may decide the electronic structure of the molecule. One motivation for investigating Ni_2,[7] Pt_2 (and eventually Pd_2) is to provide the necessary data for testing the various theoretical methods which are applied to these molecules.

Section II of this paper deals with the experimental aspects of this study, which was conducted using resonant

 0021-9606/88/215517-07$02.10

two-photon ionization spectroscopy applied to the jet-cooled platinum dimer. Section III presents our findings and relates them to previous work. In Sec. IV the results are discussed in relation to the electronic structure of Pt_2, and a summary of our conclusions is given in Sec. V.

II. EXPERIMENTAL

The molecular beam apparatus employed in our laboratory is similar to that used in previous investigations.[16,31] A pulsed supersonic beam of platinum clusters is produced by laser vaporization of a platinum disk (Johnson Matthey Aesar, 0.5 mm thick, 99.99% purity) located in the throat of a pulsed supersonic nozzle using the second harmonic light (532 nm, 100 mJ/pulse) of a *Q*-switched Nd:YAG laser (Quantel, model 580-10). The vaporization laser is timed to fire at the peak density of helium carrier gas, which is pulsed over the target by a homemade magnetically operated double solenoid valve. The high pressure of helium (8 atm in the reservoir behind the pulsed valve) in the 2 mm diameter nozzle throat insures enough three-body collisions to quench the plasma and form the platinum clusters. Cluster formation, up to Pt_{12}, is facilitated by attaching a face plate and extender to the nozzle. In order to prevent the drilling of a hole through the platinum disk, the disk is continuously rotated and translated with a mechanized assembly similar to that described in Ref. 32.

Following cluster formation, the clusters are entrained in the carrier gas and expand freely into a vacuum chamber maintained at 1×10^{-3} Torr. The resulting supersonic expansion then cools the internal degrees of freedom of the nascent clusters. The supersonic jet is collimated by a conical skimmer and subsequently enters a second vacuum chamber, which houses the ionization region of a homemade reflectron-type time-of-flight mass spectrometer. Ionization of the clusters is accomplished by resonant two-photon ionization, following which the ions are accelerated up a 0.9 m flight tube. A reflecting electric field assembly is mounted at the apex of this flight tube, thereby reflecting the ions 18° down a second flight tube. A microchannel plate detector (Galileo, model 3025-B) located at the end of the second flight tube collects the signal, which is then amplified (Pacific Instruments model 2A50), digitized by a transient recorder (Transiac, model 2001), and signal averaged by a DEC 11/73 microcomputer. The entire experiment operates under the control of this microcomputer.

Resonant two-photon ionization spectra of Pt_2 were obtained using a dye laser (Molectron, model DL-II) pumped by the second or third harmonic of a *Q*-switched Nd:YAG laser (Quantel, model 581-C) to electronically excite the platinum dimer. Following excitation, photoionization was achieved by subjecting the excited molecules to the output of an excimer laser (Questek, model 2420) operating on either the ArF (193 nm, 6.42 eV) or F_2 (157 nm, 7.89 eV) transitions. In certain regions of the spectrum, frequency summing was required to generate the appropriate excitation wavelength. This was accomplished by combining the fundamental of the Nd:YAG laser, 1064 nm, with the fundamental of the appropriate dye in a 58° KD*P Type II frequency summing crystal. The crystal was angle tuned using a homemade autotracking device. In the course of this investigation the dye laser was operated using all of the following dyes: stilbene 420, coumarins 440, 460, 480, 500, and 540A, fluorescein 548, rhodamines 590, 610, and 640, DCM, and LDS dyes 698, 750, 751, 821, and 867 (all obtained from Exciton).

III. RESULTS

A. Vibronic spectra of Pt_2

Our investigations of the jet-cooled platinum dimer reveal a large number of vibronic bands throughout the visible, extending into the near infrared and ultraviolet (11 300–26 300 cm^{-1}). In this respect the spectrum is reminiscent of that obtained for diatomic nickel,[7] which also possesses a very dense optical spectrum. In contrast to previous observations reported for Ni_2, however, the vibronic spectrum of Pt_2 displays recognizable, well-behaved vibrational progressions over most of the range studied. By carefully examining the spectrum of Pt_2, paying particular attention to the intensity patterns and isotopic shifts of the vibronic features, we have been able to identify 26 distinct band systems which are characterized in Table I by the frequency of the origin band ν_{00}, the vibrational frequency of the upper state ω'_e, and its anharmonicity $\omega'_e x'_e$. Figure 1 displays a small part of the optical spectrum of Pt_2, taken from the low-frequency portion of our scan. In this spectrum specific bands from Systems I–III are identified. It is evident from Fig. 1 that these progressions are quite regular, and this is borne out by the small error limits derived from the least-squares fits, which are listed in Table I.

In addition to locating some 26 distinct band systems, we have attempted to find hot bands, which would have enabled us to deduce the vibrational frequency of the ground electronic state. Despite careful examination of our spectra, no assignable hot bands were observed. Evidently, the excited vibrational levels of Pt_2 are effectively quenched in these experiments. Additional evidence of this is provided in Sec. III B below.

Having identified 26 distinct band systems in Pt_2, a question naturally arises: Do all of these band systems arise from the ground electronic state, or are metastable electronic states of Pt_2 present in our molecular beam? Although one cannot be absolutely definite on this point, we believe that all of the band systems listed in Table I originate from the ground electronic state of Pt_2. For these experiments our source was configured with a face plate and extender, as described in Sec. II. With this assembly, the helium and nascent clusters flow downstream from the point of vaporization through a 2 mm diameter channel 15 mm in length. At the end of this channel, the gases enter a channel 4 mm in diameter, 10 mm in length. Finally, this channel expands to 6 mm in diameter for another 5 mm in length, following which a final orifice of about 1.5 mm diameter is encountered. The original purpose of this arrangement was to introduce turbulence and lengthen the amount of time prior to the final expansion into vacuum, so that Pt_2 could be generated in greater quantity. In addition, however, this design is quite effective in quenching the internal degrees of freedom of Pt_2.

TABLE I. Band systems of Pt_2.

Band system		ν_{00}(observed)[a,b]	ν_{00}(fitted)[c]	ω'_e	$\omega'_e x'_e$
I	(6)[d]	11 426.4	11 426.58 ± 0.35	191.81 ± 0.39	0.79 ± 0.06
II	(5)	11 649.4	11 649.35 ± 0.21	187.96 ± 0.31	− 0.13 ± 0.06
III	(4)	11 767.8	11 767.83 ± 0.28	170.69 ± 0.60	0.27 ± 0.15
IV	(4)	11 816.3	11 816.45 ± 0.78	193.98 ± 1.65	1.95 ± 0.40
V	(4)	12 507.8	12 507.89 ± 0.37	185.91 ± 0.78	− 0.48 ± 0.19
VI	(4)	12 921.4	12 921.19 ± 0.72	194.61 ± 1.51	0.12 ± 0.37
VII	(4)	13 089.2	13 089.41 ± 0.72	182.94 ± 1.74	0.25 ± 0.43
VIII	(5)	13 255.5	13 255.35 ± 0.29	187.21 ± 0.43	0.21 ± 0.08
IX	(4)	13 408.6	13 408.47 ± 0.39	186.86 ± 0.82	0.60 ± 0.20
X	(5)	13 516.9	13 516.45 ± 0.79	178.38 ± 1.15	0.95 ± 0.22
XI	(7)	14 041.7	14 040.80 ± 0.88	159.90 ± 0.80	− 1.09 ± 0.11
XII	(5)	14 501.7	14 501.62 ± 1.19	146.73 ± 1.74	0.16 ± 0.34
XIII	(4)	15 297.1	15 296.94 ± 0.78	163.52 ± 1.65	− 1.50 ± 0.40
XIV	(4)	15 367.4	15 367.23 ± 0.52	145.68 ± 1.10	1.20 ± 0.27
XV	(4)	15 386.2	15 386.20 ± 0.04	153.06 ± 0.09	1.10 ± 0.02
XVI	(4)	15 954.5	15 954.45 ± 0.13	157.12 ± 0.28	0.15 ± 0.07
XVII	(4)	16 003.4	16 003.61 ± 1.11	146.63 ± 2.34	− 1.18 ± 0.57
XVIII	(4)	17 913.6	17 913.66 ± 1.47	171.33 ± 1.64	− 0.08 ± 0.27
XIX	(4)	18 345.9	18 345.82 ± 0.20	191.93 ± 0.41	2.42 ± 0.10
XX	(4)	19 751.6	19 751.81 ± 0.81	151.71 ± 1.69	− 0.58 ± 0.41
XXI	(4)	20 318.0	20 317.96 ± 0.02	148.63 ± 0.05	0.37 ± 0.01
XXII	(4)	20 374.5	20 374.20 ± 1.46	163.79 ± 3.07	0.08 ± 0.75
XXIII	(8)	20 954.0	20 953.11 ± 0.98	167.49 ± 0.74	2.79 ± 0.09
XXIV	(3)[e]	21 015.7	21 015.7	145.20	1.65
XXV	(5)	22 730.8	22 730.56 ± 0.66	140.78 ± 0.96	− 0.47 ± 0.19
XXVI	(6)	22 762.7	22 762.85 ± 0.82	140.33 ± 0.91	1.08 ± 0.15

[a] All numerical values are in wave numbers.

[b] Absolute band frequencies are measured using the $5d^8 6s(^4F)6p(^5D_4^0) \leftarrow 5d^9 6s(^3D_3)$ Pt atomic transition at 30 157.0 cm^{-1} as an internal calibration, and are expected to be accurate to within ± 5 cm^{-1}.

[c] The band origin ν_{00}, fundamental frequency ω'_e, and the anharmonicity $\omega'_e x'_e$ of the upper electronic states were obtained by fitting a linear least-squares treatment of $\nu = \nu_{00} + \omega'_e v + \omega'_e x'_e(-v - v^2)$.

[d] Quantities in parentheses are the number of band members identified for that system.

[e] Since only three bands were observed for System XXIV, ν_{00}, ω'_e, and $\omega'_e x'_e$ were uniquely determined, and no least-squares error estimate can be given. The uncertainty in the reported spectroscopic constants is expected to be comparable to that found for the other band systems.

The case of sonic flow provides a lower bound on the amount of time spent in this high-pressure region of about 30 μs. In this period of time, a Pt_2 molecule can be expected to suffer some 8×10^5 hard-sphere collisions with helium (assuming a local pressure of 2 atm). This is evidently sufficient to cool the vibrational motion of Pt_2 quite effectively, and is expected to cool the electronic degrees of freedom as well. Further cooling then occurs during the supersonic expansion into vacuum.

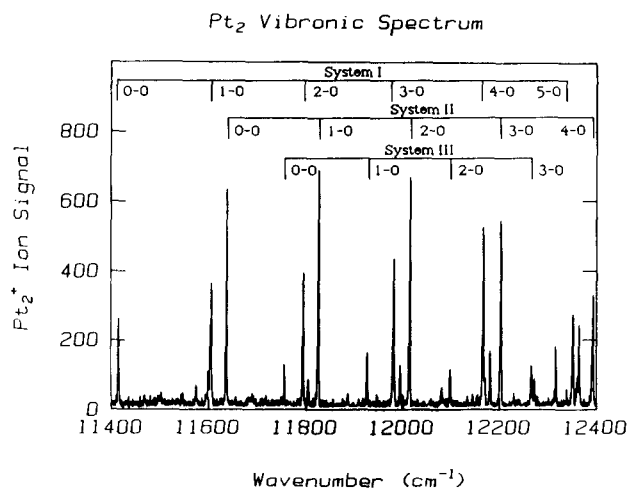

FIG. 1. Resonant two-photon ionization spectrum of Pt_2, obtained using the dyes LDS 867 and 821 to excite the molecule and the F_2 excimer laser transition (157 nm) as the ionization photon. The three lowest frequency band systems which we have observed are indicated in the figure, and their ν'_{00}, ω'_e, and $\omega'_e x'_e$ values are given in Table I. Members of band systems IV and V are also present in the figure, but these have not been labeled.

Prior to this work matrix isolation studies of diatomic platinum had been conducted by Pellin,[33] and by Jansson and Scullman.[34] Pellin has observed numerous vibronic progressions in the 600–850 nm region by dispersed fluorescence studies of matrix isolated Pt_2.[33] Jansson and Scullman have identified a particularly simple single progression in an annealed argon matrix with $\nu_{00} = 11\,247.8$ cm^{-1}, $\omega'_e = 218.1$ cm^{-1}, and $\omega'_e x'_e = 0.9$ cm^{-1}.[34] This progression appears to be quite isolated in the matrix study,[34] whereas our data show numerous vibronic systems in this spectral region. Moreover, the value of ω'_e observed in the matrix investigation is 12% higher than that obtained for any of the band systems we have observed. A matrix shift of the magnitude is quite uncommon for vibrational frequencies, except for vibrational motions of weakly bound van der Waals molecules.[35] Consequently, we do not believe that any of our band systems correlate with that observed in the matrix. The availability of near-infrared laser dyes has limited our investigation to laser frequencies above 11 300 cm^{-1}; we suspect the intense band system observed by Jansson and Scullman lies to the red of this limit in the gas phase.

B. Dissociation energy of Pt_2

The ground electronic state of atomic platinum is $5d^9(^2D_{5/2})6s$, $^3D_3$,[30] so the lowest dissociation threshold of Pt_2 corresponds to production of two $^3D_3$ platinum atoms. From this limit 28 distinct molecular electronic states arise [in Hund's case (c), which is certainly appropriate for Pt_2].[36] Some of these electronic states spin–pair both 6*s* electrons in a sigma-bonding orbital and are strongly bound, possibly correlating to the ground state. Other states arising from the $^3D_3 + {}^3D_3$ separated atom limit couple the 6*s* electrons to a spin of 1, resulting in repulsive potential energy curves. In addition to these 28 electronic states correlating to the $^3D_3 + {}^3D_3$ separated atom limit, 42 electronic states correlate to $^3D_3 + {}^3D_2$ separated atoms (0.096 eV above $^3D_3 + {}^3D_3$ atoms), 72 electronic states correlate to $^3D_3 + {}^3F_4$ separated atoms (0.102 eV above $^3D_3 + {}^3D_3$ atoms), and 15 electronic states correlate to $^3D_2 + {}^3D_2$ separated atoms (0.192 eV above $^3D_3 + {}^3D_3$ atoms).[36] As one approaches the dissociation limit of Pt_2, the number of distinct electronic states becomes very large indeed.

With 157 molecular states present within 0.2 eV of the lowest dissociation threshold, it is likely that perturbations between these states will be significant. Moreover, as soon as the lowest dissociation limit is exceeded, perturbations between these states will lead inevitably to predissociation. Thus for Pt_2, predissociation is likely to occur as soon as the lowest dissociation limit is exceeded. The occurrence of predissociation above a certain excited state energy will manifest itself by an abrupt drop in excited state lifetime. In the case of Ni_2 the excited state lifetime drops from about 10 μs to 10 ns over a range of energy of about 20 cm^{-1}; this has allowed an extraordinarily precise determination of the bond strength of the dinickel molecule.[7]

Using time-delayed resonant two-photon ionization techniques we have measured the lifetimes of many excited states of Pt_2, particularly toward the high-frequency end of our scans. Figure 2 displays a typical lifetime plot for the 23 391 cm^{-1} absorption band of Pt_2, which has been least-squares fit to an exponential decay with a lifetime of 510 $\pm$ 6 ns. Figure 3 shows the measured lifetimes for the upper states of more than 20 transitions plotted as a function of excitation energy. An abrupt drop in excited state lifetime is clearly observed at 25 336.2 $\pm$ 23 cm^{-1}. All bands to the blue of this limit exhibit lifetimes below 30 ns, while all bands to the red possess lifetimes longer than 140 ns. Although this abrupt drop in lifetime is not as dramatic as that observed for Ni_2, it nevertheless presents strong evidence for a predissociation threshold at this energy. Accordingly, we assign D_0(Pt–Pt) as 3.14 $\pm$ 0.02 eV.

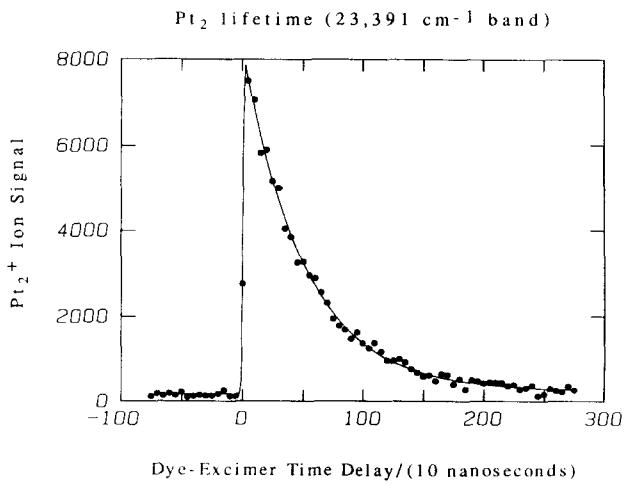

FIG. 2. Lifetime of the upper state of the 5–0 band of System XXVI of Pt_2, measured by time-delayed resonant two-photon ionization methods. In this plot the dye laser excites the Pt_2 molecule at $t = 0$, and the ArF excimer laser is fired after the indicated delay. The solid curve is a least-squares fit to the data, which gives a lifetime of 510 $\pm$ 6 ns for this state of Pt_2.

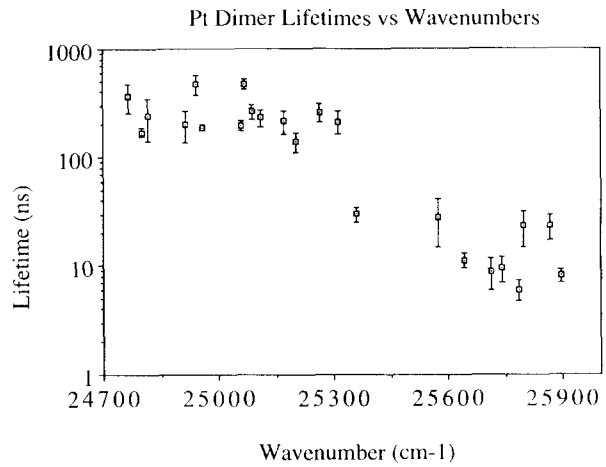

FIG. 3. Lifetimes of successive vibronic levels near the predissociation threshold of Pt_2, measured by time-delayed resonant two-photon ionization. At the predissociation threshold the measured lifetime drops from 214.5 $\pm$ 50.8 ns at 25 313.3 cm^{-1} to 30.0 $\pm$ 4.8 ns at 25 359.0 cm^{-1}. To the blue of this latter frequency, no transitions are observed with lifetimes greater than 30 ns, while no transitions to the red of this limit have lifetimes below 140 ns. For this figure, short lifetimes were least-squares fitted to a convolution of a Gaussian laser time profile and an exponential molecular decay function. This was not necessary for the long lifetimes ($\tau > 100$ ns).

The observation of a sharp predissociation threshold provides additional evidence that the diplatinum molecules probed in these experiments are vibrationally and electronically cold. If the molecular beam contained a significant population of vibrationally or electronically excited Pt_2 molecules, these species would exhibit a predissociation threshold shifted to lower frequencies by the amount of internal energy present. If this were the case we would expect to observe an energy range containing both long-lived and short-lived bands. There is no evidence in Fig. 3 of such a range, providing confirmation that the observed band systems all originate from the vibrationless level of the ground electronic state.

In previous work, Pt_2 has been investigated by Knudsen effusion mass spectrometry. Although an early investigation[37] failed to detect Pt_2, Gupta, Nappi, and Gingerich were subsequently successful in detecting Pt_2 in equilibrium with atomic platinum over the temperature range 2259–2736 K.[38] A second-law evaluation provided $D_0(Pt_2) = 3.71 \pm 0.61$ eV, while a third-law estimate gave $D_0(Pt_2) = 3.71 \pm 0.16$ eV.[38] Both estimates exceed our measurement by 0.57 eV, although our result is within the error limits of the second-law evaluation. As has been discussed elsewhere,[22] the third-law method relies on the statistical mechanical expression

for the equilibrium constant of the reaction $Pt_2 \rightleftarrows 2Pt$, in combination with measured values of this equilibrium constant, to derive a value of $D_0(Pt_2)$. To apply this method the partition function of the diatomic molecule must be calculated, and this requires knowledge of the bond length, vibrational frequency, and electronic degeneracy of all low-lying electronic states. Gupta, Nappi, and Gingerich assumed only one low-lying electronic state, a $^1\Sigma$ ground state with $r_e = 2.34$ Å and $\omega_e = 259.4$ cm^{-1} for their third-law estimate.[38] We have repeated their calculation using the low-lying electronic states reported in Table VI of Balasubramanian's paper.[36] In combination with the experimental values of K_p for the reaction $Pt_2 \rightleftarrows 2Pt$[38] this gives $D_0(Pt_2)$ 3.10 ± 0.06 eV if a symmetry number of 1 is used for Pt_2, or $D_0(Pt_2) = 3.26 \pm 0.06$ eV if a symmetry number of 2 is adopted. Rigorously, a symmetry number of 2 is only appropriate for truly homonuclear dimers, such as $^{195}Pt_2$, while a symmetry number of 1 is appropriate for heteronuclear species such as $^{195}Pt^{196}Pt$. Since 29.17% of all Pt_2 molecules are truly homonuclear, a weighted average of these results is probably most appropriate, giving $D_0(Pt_2) = 3.15 \pm 0.06$ eV. This is in excellent agreement with out result, which gives $D_0(Pt_2) = 3.14 \pm 0.02$ eV. Both values are in fair agreement with empirical estimates by Krasnov[39] (3.43 ± 0.48 eV) and Miedema and Gingerich[40] (2.88 ± 0.26 eV) as well.

C. Ionization potential of Pt_2

In the resonant two-photon ionization spectroscopy experiment, as conducted here, the first photon is absorbed from a scanning dye laser, and the second photon is absorbed from a fixed-frequency excimer laser, thereby photoionizing the molecule of interest. As the dye laser is scanned to lower energies, eventually the sum of the two-photon energies will drop below the energy required to ionize the molecule, and no more transitions will be observed. Of course, the failure to observe transitions does not prove that the sum of the two photon energies is below the ionization limit; it is possible that there are simply no absorptions in this spectral region. By repeating the scan with a higher energy ionization laser, however, one may confirm that transitions are indeed present, but cannot be observed with the less energetic ionization laser.

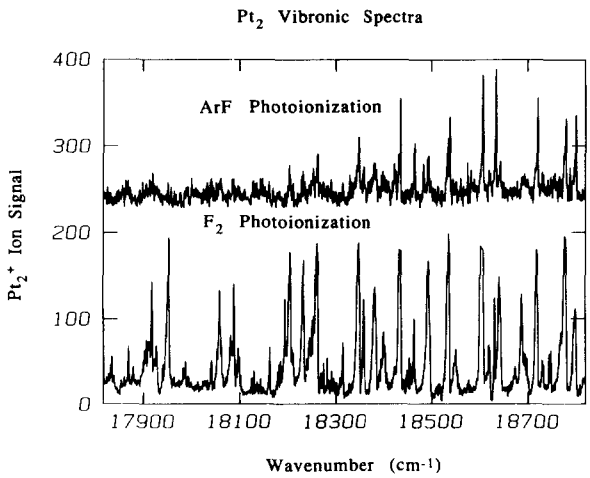

FIG. 4. Determination of the ionization threshold of Pt_2. In the upper spectrum, radiation from an ArF excimer laser (6.42 eV) is employed as the ionization photon in the R2PI scheme. The lower spectrum is obtained using F_2 excimer radiation (7.9 eV) as the ionization photon. The last band observed using the ArF radiation occurs at 18 202.0 cm^{-1}, placing the ionization potential of Pt_2 at 8.68 ± 0.02 eV. Both spectra were obtained using coumarin 540A, pumped by the third harmonic of a Nd:YAG laser, to generate the resonant photon in the R2PI process.

Figure 4 displays the results of just such an experiment. The upper scan shows the vibronic spectrum of Pt_2 in the 17 800–18 800 cm^{-1} range, obtained using ArF excimer radiation (193 nm, 6.42 eV) as the ionization laser. The lower scan shows the same spectrum obtained using F_2 radiation (157 nm, 7.90 eV) as the second color. Vibronic transitions are apparent throughout the region using the F_2 laser, but these become weaker and eventually disappear as the dye laser is scanned to the red using ArF radiation. Presumably the decrease in intensity arises because there are poor Franck–Condon factors for production of ground state, $v = 0$ ions from the intermediate states accessed in this energy range. Based on the last observed transition, located at 18 202.0 cm^{-1}, we assign the ionization potential of Pt_2 as 8.68 ± 0.02 eV.

Having measured both the bond strength and ionization potential of Pt_2, it is a simple matter to complete the thermodynamic cycle and obtain the bond strength of Pt_2^+, through the relation

$$D_0(\text{Pt–Pt}^+) = D_0(\text{Pt–Pt}) + \text{IP(Pt)} - \text{IP}(Pt_2). \quad (3.1)$$

In addition to our measured values of D_0(Pt–Pt) and IP (Pt_2), we also need the ionization potential of atomic platinum to complete this thermodynamic cycle. In Moore's tables[30] the atomic ionization potential of platinum is given as 9.0 eV, but this number is derived by fitting the $5d^96s(^3D_3)$ and $5d^97s(^3D_3)$ levels to the Rydberg formula, and correcting by the percent error expected, based on other elements which are more precisely known. Since the $5d^96s$ ($^3D_3$) level is the ground state of the platinum atom, the basis for this extrapolation is tenuous at best. In other work, an electron impact study finds an appearance potential of Pt^+ to be 8.82 ± 0.04 eV, however, this shifts to 8.61 eV when corrections are applied to account for electron impact processes which produce excited states of Pt^+.[41] In view of these results, we adopt the value IP (Pt) $= 8.80 \pm 0.20$ eV, from which we derive $D_0(\text{Pt–Pt}^+) = 3.26 \pm 0.24$ eV. This presents the interesting and unusual case of a dimer for which the ionization potential is more accurately known than is that of the constituent atoms.

IV. DISCUSSION

A major unresolved question in the chemical bonding between transition metal atoms concerns the degree of *d*-electron participation in the bonding. Little is experimentally known about such effects, but the theoretical expectations are clear[22]: (1) *d*-electron participation in the chemical bonding will become less significant as one increases the atomic number within a transition series, because the additional nuclear charge causes the *d* orbitals to contract. The outer *s* orbital is shielded more effectively from this in-

creased nuclear charge, and is less susceptible to contraction. (2) *d*-electron participation is expected to be more significant in the 4*d* and 5*d* transition metal series, because these orbitals suffer less contraction (relative to the 5*s* and 6*s*, respectively) than does the 3*d* orbital, in part due to relativistic effects.

As a result of these effects, the 3*d* contribution to the chemical bonding in Ni_2 is essentially nil. The bond strength of $Ni_2(2.068 \pm 0.01$ eV)[7] is nearly identical to that of $Cu_2(2.01 \pm 0.08$ eV).[22] Likewise, Ni_2 and Cu_2 have almost identical bond lengths (2.20 [7] and 2.2195 Å,[42,43] respectively). The situation is quite different among the 5*d* transition metal dimers, however. Our measured bond strength of $Pt_2(3.14 \pm 0.02$ eV) is substantially stronger than that measured for $Au_2(2.29 \pm 0.02$ eV),[44] indicating significant participation of the 5*d* electrons in the chemical bonding of Pt_2.

In an early *ab initio* investigation of Ni_2, Pd_2, and Pt_2, Basch, Cohen, and Topiol found little or no *d* orbital contribution to the bonding in Ni_2 and Pd_2, but substantial 5*d* contributions in Pt_2.[45] These authors used a relativistic effective core potential to limit the number of electrons actively considered, and then applied a multiconfiguration self-consistent-field treatment to several representative states arising from the $(6s\sigma_g)^2 5d^9_A 5d^9_B$ electronic configuration of Pt_2. Correlation of the bonding (σ) electrons was built into the calculation, but other correlations among the open *d*-shell electrons were omitted. Spin–orbit effects were also ignored. These limits to the calculation cause a drastic underestimate of the Pt_2 bond strength, predicting $D_0(Pt_2) = 0.93$ eV for a $^1\Gamma_g$ state which places both *d*-shell holes in δ orbitals.[45]

More recently, Balasubramanian has investigated Pt_2 using a relativistic core potential method to describe the $[Xe]4f^{14}$ cores, along with a complete active space self-consistent-field treatment of the remaining 20 electrons (d^9s^1–d^9s^1).[36] Following the CASSCF calculation, additional correlation effects were included by a first-order configuration interaction treatment, after which the spin–orbit interaction was introduced. This monumental effort represents the most detailed theoretical investigation of an open 5*d*-shell transition metal dimer reported to date. Despite this effort, a bond strength of 2.31 eV is obtained ignoring spin–orbit coupling. With spin–orbit coupling included this drops to 1.97 eV, and completely rearranges the energy ordering among the electronic states. Evidently, considerable additional electronic correlation is required to bring the calculated value of $D_0(Pt_2)$ into agreement with experiment.

Although the high value of $D_0(Pt_2)$ provides the strongest evidence of significant *d*-orbital participation in the chemical bonding of Pt_2, additional support for this idea may be found in the vibronic spectrum itself. If the *d* orbitals were contracted so tightly that they did not take part in the chemical bonding, one would expect very slight differences in the orbital energies of the $d\sigma$, $d\pi$, and $d\delta$ orbitals. On the other hand, these orbital energies would be expected to be widely separated if there were significant *d*–*d* interactions between the two metal atoms. Diatomic nickel conforms to the former expectation, resulting in an extremely congested vibronic spectrum with spectral features occurring with an average spacing of 10 cm^{-1}.[7] In Pt_2, however, the average spacing between vibronic features is perhaps 40 or 50 cm^{-1}, resulting in a spectrum which is interpretable. The decreased density of electronic states in Pt_2 arises in part because the *d*-orbital splittings in this species are significantly greater than in Ni_2; in addition, the greater spin–orbit splitting in Pt_2 contributes to a decreased electronic state density as well.

V. CONCLUSION

A resonant two-photon ionization spectroscopic investigation of jet-cooled Pt_2 has revealed numerous vibronic bands throughout the visible, extending into the near infrared and ultraviolet regions of the spectrum. Although the spectrum is dense, 26 vibronic progressions have been identified and characterized by ν_{00}, ω'_e, and $\omega'_e x'_e$. The onset of predissociation, inferred from an abrupt drop in excited state lifetime, has been used to determine $D_0(Pt_2) = 3.14 \pm 0.02$ eV. This is consistent with high-temperature Knudsen effusion studies, provided the partition function of Pt_2 is reevaluated using *ab initio* results for the low-lying electronic states of the dimer.

In addition to these measurements, a comparison of the optical spectra generated using ArF and F_2 excimer radiation as the ionization photon has permitted a measurement of the ionization potential of Pt_2, which is determined to be 8.68 ± 0.02 eV. In combination with the measured bond strength of Pt_2 and the ionization potential of atomic platinum, this places the bond strength of Pt_2^+ at 3.26 ± 0.24 eV.

Finally, we note that the bond strength of Pt_2 is significantly greater than that of Au_2, demonstrating the importance of 5*d* contributions to the chemical bond in this species.

Attempts are currently in progress to extend this investigation to the congeneric Pd_2 molecule, which is expected to be much less strongly bound. In addition, efforts are currently under way to construct a single-mode, transform-limited pulsed dye laser, which should enable the investigation of the observed spectra with rotational resolution.

ACKNOWLEDGMENTS

We are grateful to Professor Edward M. Eyring for the gift of some platinum foil, which was used in this work. We also gratefully acknowledge research support from the National Science Foundation, under Grant No. CHE-85-21050.

[1] J. L. Gole, J. H. English, and V. E. Bondybey, J. Phys. Chem. **86**, 2560 (1982).
[2] D. R. Preuss, S. A. Pace, and J. L. Gole, J. Chem. Phys. **71**, 3553 (1979).
[3] V. E. Bondybey, G. P. Schwartz, and J. H. English, J. Chem. Phys. **78**, 11 (1983).
[4] E. A. Rohlfing and J. J. Valentini, J. Chem. Phys. **84**, 6560 (1986).
[5] D. E. Powers, S. G. Hansen, M. E. Geusic, A. C. Puiu, J. B. Hopkins, T. G. Dietz, M. A. Duncan, P. R. R. Langridge-Smith, and R. E. Smalley, J. Chem. Phys. **86**, 2556 (1982).
[6] D. E. Powers, S. G. Hansen, M. E. Geusic, D. L. Michalopoulos, and R. E. Smalley, J. Chem. Phys. **78**, 2866 (1983).

[7]M. D. Morse, G. P. Hansen, P. R. R. Langridge-Smith, L.-S. Zheng, M. E. Geusic, D. L. Michalopoulos, and R. E. Smalley, J. Chem. Phys. **80**, 5400 (1984).
[8]P. J. Brucat, L.-S. Zheng, C. L. Pettiette, S. Yang, and R. E. Smalley, J. Chem. Phys. **84**, 3078 (1986).
[9]A. D. Sappey, J. E. Harrington, and J. C. Weisshaar, J. Chem. Phys. **88**, 5243 (1988).
[10]D. G. Leopold, J. Ho, and W. C. Lineberger, J. Chem. Phys. **86**, 1715 (1987).
[11]O. Cheshnovsky, P. J. Brucat, S. Yang, C. L. Pettiette, M. J. Craycraft, and R. E. Smalley, in *Physics and Chemistry of Small Clusters*, edited by P. Jena, B. K. Rao, and S. N. Khanna (Plenum, New York, 1987), NATO ASI Series B: Physics,Vol. 158, p. 1.
[12]D. J. Trevor, R. L. Whetten, D. M. Cox, and A. Kaldor, J. Am. Chem. Soc. **107**, 518 (1985).
[13]S. C. Richtsmeier, E. K. Parks, K. Liu, L. G. Pobo, and S. J. Riley, J. Chem. Phys. **82**, 3659 (1985).
[14]M. D. Morse, M. E. Geusic, J. R. Heath, and R. E. Smalley, J. Chem. Phys. **83**, 2293 (1985).
[15]R. J. St. Pierre and M. A. El.-Sayed, J. Phys. Chem. **91**, 763 (1987).
[16]Y. Hamrick, S. Taylor, G. W. Lemire, Z.-W. Fu, J.-C. Shui, and M. D. Morse, J. Chem. Phys. **88**, 4095 (1988).
[17]K. Ervin, S. K. Loh, N. Aristov, and P. B. Armentrout, J. Phys. Chem. **87**, 3593 (1983).
[18]P. B. Armentrout, S. K. Loh, and K. M. Ervin, J. Am. Chem. Soc. **106**, 1161 (1984).
[19]M. F. Jarrold, A. J. Illies, and M. T. Bowers, J. Am. Chem. Soc. **107**, 7339 (1985).
[20]D. B. Jacobson and B. S. Freiser, J. Am. Chem. Soc. **107**, 1581 (1985).
[21]W. Weltner, Jr. and R. J. Van Zee, Annu. Rev. Phys. Chem. **35**, 291 (1984).
[22]M. D. Morse, Chem. Rev. **86**, 1049 (1986).
[23]D. R. Salahub, in *Ab Initio Methods in Quantum Chemistry II*, edited by K. P. Lawley (Wiley, New York, 1987); Adv. Chem. Phys. **69**, 447 (1987).
[24]S. P. Walch and C. W. Bauschlicher, Jr., in *Comparison of Ab Initio Quantum Chemistry with Experiment*, edited by R. J. Bartlett (Reidel, Dordrecht, 1985), p. 17.
[25]W. Weltner, Jr. and R. J. Van Zee, in *Comparison of Ab Initio Quantum Chemistry with Experiment*, edited by R. J. Bartlett (Reidel, Dordrecht, 1985), p. 1.
[26]D. J. Trevor and A. Kaldor, in *High Energy Processes in Organometallic Chemistry*, edited by K. S. Suslick, ACS Symp. Ser. **333** (American Chemical Society, Washington, D.C., 1987), p. 43.
[27]A. Kaldor, D. M. Cox, and M. R. Zakin, Adv. Chem. Phys. (in press).
[28]S.-S. Lin, B. Strauss, and A. Kant, J. Chem. Phys. **51**, 2282 (1969).
[29]I. Shim and K. A. Gingerich, J. Chem. Phys. **80**, 5107 (1984).
[30]C. E. Moore, Natl. Bur. Stand. Circ. No. 467 (1971), Vol. III.
[31]Z.-W. Fu, G. W. Lemire, Y. Hamrick, S. Taylor, J.-C. Shui, and M. D. Morse, J. Chem. Phys. **88**, 3524 (1988).
[32]S. C. O'Brien, Y. Liu, Q. Zhang, J. R. Heath, F. K. Tittel, R. F. Curl, and R. E. Smalley, J. Chem. Phys. **84**, 4074 (1986).
[33]M. J. Pellin (unpublished results).
[34]K. Jansson and R. J. Scullman, J. Mol. Spectrosc. **61**, 299 (1976).
[35]M. E. Jacox, J. Mol. Spectrosc. **113**, 286 (1985).
[36]K. Balasubramanian, J. Chem. Phys. **87**, 6573 (1987).
[37]J. H. Norman, H. G. Staley, and W. E. Bell, J. Phys. Chem. **71**, 3686 (1967).
[38]S. K. Gupta, B. M. Nappi, and K. A. Gingerich, Inorg. Chem. **20**, 966 (1981).
[39]R. S. Krasnov, Teplofiz. Vys. Temp. **13**, 441 (1975).
[40]A. R. Miedema and K. A. Gingerich, J. Phys. B **12**, 2081 (1979).
[41]E. G. Rauh and R. J. Ackermann, J. Chem. Phys. **70**, 1004 (1979).
[42]N. Åslund, R. F. Barrow, W. G. Richards, and D. N. Travis, Ark. Fys. **30**, 171 (1965).
[43]T. V. R. Rao and S. V. J. Lakshman, J. Quant. Spectrosc. Radiat. Transfer **11**, 1157 (1971).
[44]J. Kordis, K. A. Gingerich, and R. J. Seyse, J. Chem. Phys. **61**, 5114 (1974).
[45]H. Basch, D. Cohen, and S. Topiol, Isr. J. Chem. **19**, 233 (1980).